Optical and magneto-optical properties of Gd monochalcogenides

2003 J. Phys.: Condens. Matter 15 7095

(http://iopscience.iop.org/0953-8984/15/41/017)

INSTITUTE OF PHYSICS PUBLISHING JOURNAL OF PHYSICS: CONDENSED MATTER

J. Phys.: Condens. Matter **15** (2003) 7095–7102 PII: S0953-8984(03)68037-9

Optical and magneto-optical properties of Gd monochalcogenides

Dipta Bhanu Ghosh, Molly De and S K De

Department of Materials Science, Indian Association for the Cultivation of Science, Jadavpur, Kolkata 700 032, India

Received 22 August 2003
Published 3 October 2003
Online at stacks.iop.org/JPhysCM/15/7095

Abstract

The electronic structure of Gd monochalcogenides are investigated theoretically using the full potential linear muffin-tin orbital method. The on-site Coulomb interaction (U) is accounted for by the local spin-density approximation. These calculations corroborate the fact that they are all metallic. Magnetism is driven by the spin exchange mechanism only. A deep minimum in the reflectivity spectrum occurs in GdS and GdSe. The largest Kerr rotation among the Gd monochalcogenides, of about $-5°$, is found at the shoulder followed by a rotation of about 4° at the plasma resonance energy. Both the plasma resonance and the shoulder effect are equally responsible for the moderately large magneto-optical signals in Gd monochalcogenides. A reasonably good agreement between theory and experiment is obtained.

1. Introduction

The electronic structure of rare earth (RE) compounds has been the focus of attention for some time now due to the unusual behaviour of their physical properties. Much has been done on the lighter and heavier RE compounds [1–8]. Most RE compounds exhibit a rich variety of phenomena, like the heavy fermion behaviour, intermediate valence, magnetic anisotropy, intriguing magnetic phase diagrams and the Kondo effect. One of the underlying reasons behind this is the strong correlation among the 4f electrons of the RE ion. The most significant magnetic and optical phenomenon that some RE compounds exhibit is the magneto-optical Kerr effect (MOKE). It acts as an effective probe for the 4f band states. The discovery of giant Kerr rotation of about 90° in CeSb and of 22° in CeS demanded a fresh look at the complex nature of the 4f states and the magnetic and magneto-optical properties of RE compounds [7, 8]. Earlier it was thought that the MOKE has its origin in the magnetic properties of the sample. However, the large Kerr rotation in CeS and other RE materials with a small magnetic moment proves that the explanation is not all that trivial. In the search for the origin of the MOKE, spin polarization, orbital polarization and spin–orbit coupling have been known to play vital roles. That plasma resonance [5, 7–10] is also an important factor for the magneto-optical signal has

0953-8984/03/417095+08$30.00

been established both theoretically and experimentally. In this respect our aim here is to study systems with half-filled 4f orbitals in which the orbital moment is quenched, where at least one of the factors which was earlier thought to be essential for MOKE is excluded.

Eu or Gd compounds are the ideal systems in order to study the sole effect of the exchange interaction on the electronic structure and optical properties of these compounds. The Eu monochalcogenides were studied [11] very extensively in the 1960s and 1970s. But, due to their colossal magneto-resistance, Eu monochalcogenides continue to be the focus of attention at present [12, 13]. The Gd monochalcogenides are the metallic counterpart of the Eu monochalcogenides and should be investigated thoroughly if one needs to understand the half-filled 4f systems. We are not aware of any comprehensive band structure calculations on Gd monochalcogenides (GdX, X = S, Se, Te). The experimental work [14] on which we will rely heavily on dates back to the 1970s and dealt with the effect of non-stoichiometry on reflectivity. The Gd ion is trivalent in all GdX. They are all metallic and have an antiferromagnetic ground state [15, 16]. The Néel temperatures are 62, 60.5 and 82 K for $Gd_{0.988}S$, $GdSe_{0.999}$ and $Gd_{0.993}Te$, respectively [16]. The metallic character is caused by the almost free d electrons of the RE ion. The reflectivity spectra of GdX reveal a typical metallic behaviour, i.e. a high value ($\sim 100\%$ as $\omega \rightarrow 0$) followed by a deep minimum. The reflectivity measurements show the occupied 4f state to lie about 9 eV below E_F. On analysis, the authors argue that the bottom of the conduction band is mainly of 5d character. The p states of the chalcogen lie between 7 and 3 eV below E_F. The iso-structural Ce, Nd and Tm monochalcogenides have shown fairly large MO signals [1, 2, 8]. However, the MOKE in GdX has not been studied either by experimentalists or by computational physicists. The main purpose of the present work is to investigate the electronic and magneto-optical properties of GdX from first-principles electronic structure calculations.

The first step towards determining the optical properties is the calculation of the correct band structure of GdX. The strong correlations among the 4f electrons had to be taken into account. This proves the conventional LSDA to be inadequate for studying the correlation effects of f electrons. A large Kerr rotation of about $-5°$ at about 0.4 eV has been calculated [5] in PrSb by the LSDA+U method. The results using SIC [4] or LSDA+U [1–3, 5] are definitely an improvement over the LSDA calculations. The LSDA + U magneto-optical properties and the Kerr and Faraday rotation spectra have shown good agreement with experimental results in almost all RE compounds. The LSDA+U formalism has also been found to work very well for compounds which do not contain f electrons too. The electronic structure of Mott–Hubbard insulator compounds [17], like Fe_3O_4 and the heavy-fermion compound YbBiPt [6], have been well reproduced by the LSDA + U method. Hence we adopted the LSDA + U method to study the band structure and optical properties of GdX.

2. Calculational details

Full potential (FP) self-consistent spin-polarized band structure calculations have been performed on Gd monochalcogenides GdX (X = S, Se, Te) by the linear muffin-tin orbital method (LMTO) [18] using the FP-LMTO code developed by Savrasov *et al* [19]. The density functional formalism is modified in order to include the strong correlations between the f electrons. In the LSDA+U method [20], the LSDA energy functional is modified by removing the LSDA f–f interactions and adding the strong on-site Coulomb interactions between the f electrons. The antiferromagnetic calculations proved to be very unstable with respect to the ferromagnetic calculations. The instability in the calculations suggests that we cannot rely on the total energy to prove the stability of a particular magnetic ordering. We have presented here results for the ferromagnetic calculations only. For the theoretical details of the calculation, we refer to our previous paper [5].

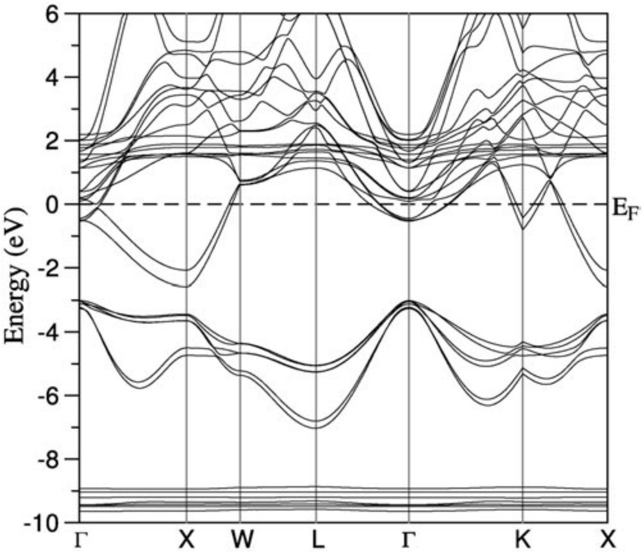

Figure 1. Band structure of GdS.

The f states [14, 21] of GdS have been found to lie 9 eV below the Fermi level, E_F. To suitably adjust the position of the f states the value of F^0 $(=U)$ is chosen to be 7 eV. The other Slater integrals F^2, F^4 and F^6 for f electrons have been used from the experimental paper by Thole *et al* [22] to calculate the matrices $U_{mm'}$ and $J_{mm'}$. The exchange correlation potential in the LSDA was calculated with Vosko–Wilk–Nussair parametrization. The experimental [14] lattice parameters for all the GdX are given in table 1. They have the rock-salt type structure at ambient conditions. The basis consists of Gd: 6s, 5p, 5d, 4f and chalcogen: (n)s, (n)p and (n)d, where n refers to the principal quantum number. The 5s electrons of Gd and $(n-1)$d electrons of Te were treated in a separate panel and hence were not included in the optical calculations. The charge density, density of states and momentum matrix elements were calculated on a grid of 242$\boldsymbol{k}$ points in an irreducible Brillouin zone and the $\boldsymbol{k}$ space integration was performed using the tetrahedron method. We have treated the orbital momentum quantum number, m_l, as a parameter and started our calculations with all the 4f^7 electrons to be occupied. This implies that we started our self-consistent calculation by treating the Gd ion as trivalent.

3. Results and discussion

The self-consistent FP band structures of Gd monochalcogenides are very similar in nature except that the characteristics change due to the increase of the chalcogen's atomic number. In figure 1, the band structure for GdS along the major symmetry directions is given. The 4f states of Gd are divided into lower and upper Hubbard bands due to the strong on-site Coulomb interaction parameter, U. The 4f occupied bands are located about 9 eV below E_F and are fully localized. Strong spin polarization couples with the strong Coulomb repulsion to lower these bands by 9 eV. The 4f unoccupied states are bunched together at about 2 eV above the E_F. The valence band also consists of the 3p bands of sulfur which are fairly wide and extend from 3 to 7 eV below E_F. At the Fermi level, the 5d bands of Gd make several crossings. The conduction band is comprised of the upper 4f Hubbard band hybridizing with the 5d bands of Gd. The band structures for GdSe and GdTe are not shown here. The p bands of the chalcogen

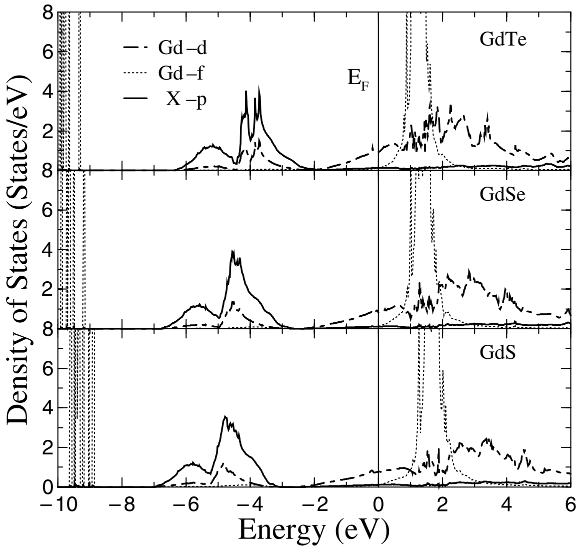

Figure 2. *l*-projected density of states of GdX (X = S, Se, Te).

Table 1. This shows a, the lattice parameter, the muffin-tin radii of Gd, S_{Gd} and chalcogen, S_{X}, the density of states at the Fermi level, $N(E_{\mathrm{F}})$, the experimental reflectivity minimum energy [14], $R_{\mathrm{min}}^{\mathrm{expt.}}$ (for $\mathrm{GdS}_{0.94}$, $\mathrm{GdSe}_{0.95}$ and GdTe) and the theoretical reflectivity minimum energy, $R_{\mathrm{min}}^{\mathrm{th.}}$.

	a (au)	S_{Gd} (au)	S_{X} (au)	$N(E_{\mathrm{F}})$ (St./eV)	$R_{\mathrm{min}}^{\mathrm{expt.\,a}}$ (eV)	$R_{\mathrm{min}}^{\mathrm{th.}}$ (eV)
GdS	10.490	2.832	2.412	0.954	3.4	3.15
GdSe	10.914	2.892	2.564	1.042	2.8	2.84
GdTe	11.572	2.950	2.835	1.205	2.0	2.65

[a] Reference [14].

show increased splitting and widening as the chalcogen size increases. The 5d bands shrink as the lattice parameter increases from GdS to GdTe. The 4f occupied band stays 9–10 eV below the Fermi level and the unoccupied 4f band moves towards E_{F} with the increase in the lattice parameter, keeping the separation between them almost equal.

Table 1 also provides information on the density of states at E_{F} and the energetic positions of experimental and theoretical reflectivity minima for all GdX. Figure 2 shows the density of states of GdX (X = S, Se, Te). The occupied 4f states do not hybridize with any other states below E_{F} and are fully separated from other bands. The spin–orbit splitting of the p bands of the chalcogen increases from S to Te. These p bands hybridize with the 5d states of Gd, as is evident from the partial DOS in figure 2. The positions of the S p band and Gd 4f lower Hubbard band are in excellent agreement with the photoelectron spectroscopic spectrum [21] of GdS. That the character of the bottom of the conduction band is 5d finds support in the experimental evidence too. The density of states at E_{F}, as given in table 1, implies the metallic nature of these compounds. The information on the spin and orbital moment due to each atom and the total magnetic moment in all the Gd monochalcogenides is given in table 2. There is a fair amount of agreement with the experimental magnetic moment [16]. The total moment is around 7 μ_{B} for all of them and is consistent with a half-filled 4f state. The orbital moment due to Gd ions is considerably smaller than the spin contribution, though not quenched. The

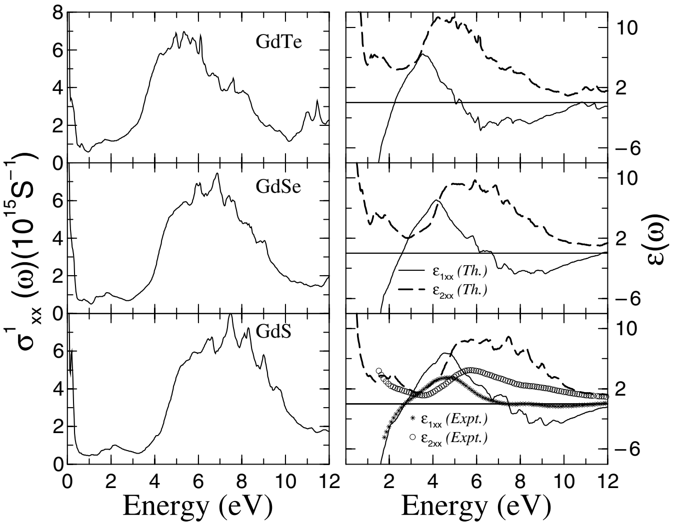

Figure 3. The calculated real component of the diagonal optical conductivity and dielectric function of GdX and the corresponding experimental [14] dielectric function spectra for $GdS_{0.94}$.

Table 2. This shows m_o and m_s, the atomic orbital and spin moments, respectively, and the total moment, $m_s + m_o$.

	m_s (Gd) (μ_B)	m_s (X) (μ_B)	m_o (Gd) (μ_B)	m_o (X) (μ_B)	$m_s + m_o$ (μ_B)
GdS	6.91	−0.02	0.09	0.00	6.98
GdSe	6.93	−0.02	0.08	0.00	6.99
GdTe	6.97	−0.03	0.08	0.00	7.02

spin moment is solely due to the spin polarization of the 4f electrons. The contribution of the chalcogen ion to the magnetic moment is negligible.

The optical conductivity tensor has been calculated from the standard relations given by Reim and Schoenes [23]. The imaginary component of the diagonal optical conductivity (σ^2_{xx}) and the real component of the off-diagonal conductivity (σ^1_{xy}) have been calculated using the Kramers–Kronig transformation. The magneto-optical Kerr rotation is calculated from the relation

$$\Phi_k = \theta_k(\omega) + i\epsilon_k(\omega) \approx \frac{-\sigma_{xy}}{\sigma_{xx}\sqrt{1 + \frac{4\pi i}{\omega}\sigma_{xx}}} \tag{1}$$

where σ_{xx} and σ_{xy} are the diagonal and off-diagonal components of the optical conductivity tensor, provided both are small and $|\sigma_{xy}| \ll |\sigma_{xx}|$. Here θ_k and ϵ_k are the Kerr rotation and Kerr ellipticity, respectively.

Optical and magneto-optical spectra have been calculated for all the GdX using the LMTO band structure and furthermore a Lorentzian broadening of about 0.0136 eV has been used. Figure 3 shows the calculated real part of the diagonal optical conductivity spectrum of GdX and the corresponding dielectric function. Conductivity spectra show a Drude minimum followed by a small structure and then a plasma minimum and a broad structure between 4 and 10 eV in all GdX. The plasma minimum appears at 3.25, 2.78 and 2.24 eV in GdS, GdSe and GdTe respectively. This minimum is not very pronounced in GdTe compared to that in the other two. One finds the same features in the imaginary part of the dielectric function. The absolute value

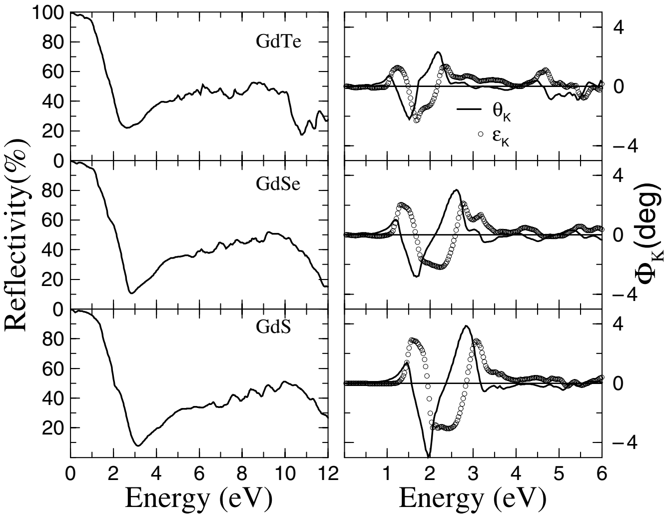

Figure 4. Calculated reflectivity spectra and Kerr spectra of GdX.

of the plasma resonance frequency is given by the real part of the dielectric function, $\epsilon^1(\omega) = 0$. From the real dielectric function spectra, plasma resonance is found to occur at 2.73, 2.6 and 2.23 eV in GdS, GdSe and GdTe, respectively. This agrees fairly well with the experimental value of the coupled plasmon mode frequencies [14] except for GdTe. Beckenbaugh *et al* [14] pointed out that interband transitions occur only after the plasma minimum. However, our calculations reveal that the small structure, which we shall call here a shoulder, between the Drude minimum and plasma minimum is due to Gd d $\rightarrow$ Gd f transitions. This transition occurs at about 2.1, 1.75 and 1.6 eV for GdS, GdSe and GdTe, respectively. In fact, the experimental spectrum [14] (ϵ^2_{xx}) of $GdS_{0.94}$ in figure 3 shows a shoulder effect between 2 and 3 eV. The broad structure centred at 7 eV in GdS is due mainly to chalcogen p to Gd d states in the conduction band. Down the chalcogen series, both the structures at 2.0 and 8.0 eV move towards lower energy. This is due to the shifting of the 4f unoccupied bands to E_F and the shrinkage of the 5d bands, which in turn is due to the increase in the lattice parameter.

The calculated reflectivity spectra of GdX are shown in figure 4. They exhibit the typical metallic behaviour since reflectivity $\rightarrow$ 100% as $\omega \rightarrow 0$ in all of them. But the Drude nature is perturbed by the structure (for example, at 2.0 eV in GdS) due to the d to f transition. This feature is not discussed in the experimental paper [14]. All but GdTe show the deep minima effect. The edge effect is considerably pronounced in GdS and GdSe and occurs at about 3.15 and 2.84 eV, respectively. GdTe shows a moderate plasma edge effect at about 2.65 eV. The reflectivity minimum occurs at energies quite near the plasma minimum and not far from the plasma resonance frequencies. This lowering in energy of the reflectivity minimum occurs due to the decrease in the indirect gap between the X p and Gd d states, which in turn is due to the widening of the p atomic wavefunctions as one goes to the higher chalcogens. The experimental and theoretical reflectivity minima positions are given in table 1. There is overall agreement about the nature of the spectrum except for the second minima (experimental) [14] for GdTe near 8 eV, which is at about 11 eV in the theoretical spectrum. This mismatch at high energies has been very common in LSDA + U calculations [1, 2, 5]. Optical conductivity calculations have been performed up to 30 eV for maximum accuracy in calculating $\sigma^2_{xx}(\omega)$ and $\sigma^1_{xy}(\omega)$.

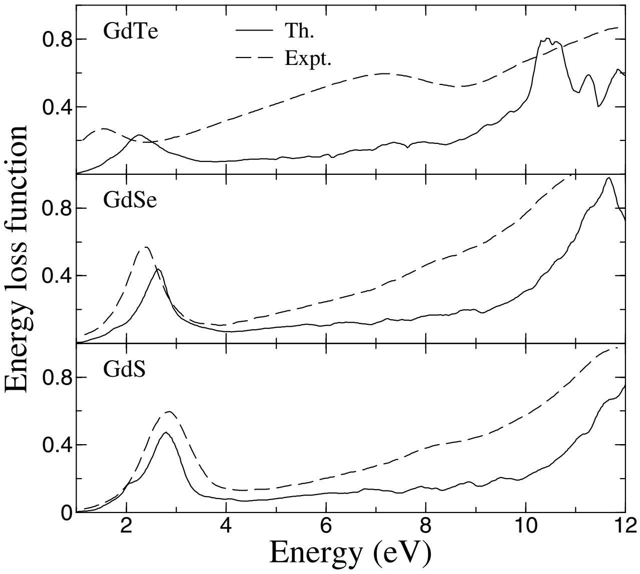

Figure 5. Calculated energy loss function of GdX and the corresponding experimental [14] spectra for $GdS_{0.94}$, $GdSe_{0.95}$ and GdTe.

Figure 4 also depicts calculated polar Kerr rotation and ellipticity. Kerr rotation is a manifestation of many phenomena. Spin polarization, spin–orbit interaction, plasma minima or edge effect, joint density of states, momentum matrix elements and orbital polarization all play important roles in determining the magneto-optical Kerr spectra. The polar Kerr rotation spectrum will follow the off-diagonal conductivity spectrum since the latter carries all the information regarding the spin polarization, spin–orbit interaction and the interaction between the two. But recent LSDA + U calculations on RE monochalcogenides and monopnictides point to plasma resonance as the most crucial ingredient in the Kerr rotation phenomenon. In this rare case, we can safely rule out orbital polarization as a factor for MOKE because of the almost negligible value of the orbital moment. A strong plasma resonance effect can be seen in GdS and GdSe. The effect is less pronounced in GdTe. As a result, the Kerr rotations are larger in GdS and GdSe. These large signals range from $-5°$ to $4°$ between 1.9 and 3 eV in GdS, $-2.9°$ to $3°$ between 1.6 and 2.6 eV in GdSe and about $-2.3°$ to $2.3°$ between 1.5 and 2.2 eV in GdTe. In other words, the largest Kerr rotation is seen between the energy at which the d to f transition or the shoulder occurs and the energy at which plasma resonance occurs. The origin of the large magneto-optical Kerr rotations lies in the pronounced plasma edge effect and the small shoulder effect in Gd monochalcogenides. This phenomenon has been seen in CeSb [7] and Nd monochalcogenides [1]. Figure 5 shows the calculated and experimental energy loss function of GdX. The spectra show pronounced structures at the plasma minima and agree very well with the experimental counterpart in GdS and GdSe.

4. Conclusion

The comprehensive electronic structure calculations on Gd monochalcogenides throw light on the description and treatment of f electrons. Excellent agreement for electronic structure and optical spectra is found with experimental results. The present work establishes that the inclusion of the on-site Coulomb interaction (U) in LSDA is essential for obtaining the correct electronic structure and optical properties of Gd monochalcogenides. The magnetic moment is only from the 4f spin. The deep minimum in the reflectivity spectra occurs in GdS and GdSe. This along with a small shoulder, gives rise to the moderately large polar Kerr rotation. Hence it can be concluded that the magneto-optical Kerr phenomenon in Gd monochalcogenides at least is due to the plasma resonance effect and the shoulder effect of primarily the 5d → 4f transition.

Acknowledgment

This work is funded by the Department of Science and Technology, Government of India (project no SP/S2/M-50/98).

References

[1] Antonov V N, Harmon B N, Perlov A Y and Yaresko A N 1999 *Phys. Rev.* B **59** 14561

[2] Antonov V N, Harmon B N and Yaresko A N 2001 *Phys. Rev.* B **63** 205112

[3] Antonov V N, Harmon B N and Yaresko A N 2002 *Phys. Rev.* B **66** 165208

[4] Svane S, Temmerman W and Szotek Z 1999 *Phys. Rev.* B **59** 7888
Svane S, Szotek Z, Temmerman W M, Laegsgaard J and Winter H 1998 *J. Phys.: Condens. Matter* **10** 5309

[5] Ghosh D B, De M and De S K 2003 *Phys. Rev.* B **67** 035118

[6] Oppeneer P M, Antonov V N, Yaresko A N, Perlov A Y and Eschrig H 1997 *Phys. Rev. Lett.* **78** 4079

[7] Pittini R, Schoenes J, Vogt O and Wachter P 1996 *Phys. Rev. Lett.* **77** 944

[8] Pittini R, Schoenes J and Wachter P 1997 *Phys. Rev.* B **55** 7524

[9] Feil H and Haas C 1987 *Phys. Rev. Lett.* **58** 65

[10] De A and Puri A 2002 *J. Appl. Phys.* **92** 5401

[11] Cho S J 1970 *Phys. Rev.* B **1** 4589

[12] Steeneken P G, Tjeng L H, Elfimov I, Sawatzky G A, Ghiringhelli G, Brookes N B and Huang D-J 2002 *Phys. Rev. Lett.* **88** 047201

[13] Schiller R and Nolting W 2001 *Solid State Commun.* **118** 173

[14] Beckenbaugh W, Evers J, Gunterodt G, Kaldis E and Wachter P 1975 *J. Phys. Chem. Solids* **36** 239

[15] Holtzberg F, McGuire T R, Methfessel S and Suits J C 1964 *Phys. Rev. Lett.* **13** 18

[16] Hulliger F and Siegrist T 1979 *Z. Phys.* B **35** 81

[17] Antonov V N, Harmon B N, Antropov V P, Perlov A Y and Yaresko A N 2001 *Phys. Rev.* B **64** 134410
Antonov V N, Harmon B N and Yaresko A N 2003 *Phys. Rev.* B **67** 024417

[18] Andersen O K 1975 *Phys. Rev.* B **12** 3060

[19] Savrasov S Y and Savrasov D Y 1992 *Phys. Rev.* B **46** 12181
Savrasov S Y 1996 *Phys. Rev.* B **54** 16470

[20] Anisimov V I, Zaanen J and Andersen O K 1991 *Phys. Rev.* B **44** 943
Lichtenstein A I, Anisimov V I and Zaanen J 1995 *Phys. Rev.* B **52** R5467

[21] Eastman D E and Kuznietz M 1971 *J. Appl. Phys.* **42** 1396

[22] Thole B T, Van der Laan G, Fuggle J C, Sawatzky G A, Karnatak R C and Esteva J M 1985 *Phys. Rev.* B **32** 5107

[23] Reim W and Schoenes J 1990 *Ferromagnetic Materials* vol 5, ed E P Wohlfarth and K H J Buschow (Amsterdam: North-Holland) p 133